Journal of Organometallic Chemistry 694 (2009) 1826–1833

Contents lists available at ScienceDirect

Journal of Organometallic Chemistry

journal homepage: www.elsevier.com/locate/jorganchem

Amino acid-functionalized cyclopentadienyl molybdenum tricarbonyl complex and its use in catalytic olefin epoxidation

Marta Abrantes [a,*], Filipe A. Almeida Paz [b], Anabela A. Valente [b], Cláudia C.L. Pereira [b,c], Sandra Gago [b], Alírio E. Rodrigues [a], Jacek Klinowski [d], Martyn Pillinger [b], Isabel S. Gonçalves [b]

[a] Laboratory of Separation and Reaction Engineering, Associate Laboratory LSRE/LCM, Faculdade de Engenharia da Universidade do Porto, Rua Dr. Roberto Frias, 4200-465 Porto, Portugal
[b] Department of Chemistry, CICECO, University of Aveiro, 3810-193 Aveiro, Portugal
[c] Unidade de Ciências Químicas e Radiofarmacêuticas, Instituto Tecnológico e Nuclear, Estrada Nacional 10, 2686-953 Sacavém, Portugal
[d] Department of Chemistry, University of Cambridge, Lensfield Road, CB2 1EW Cambridge, United Kingdom

ARTICLE INFO

Article history:
Received 26 November 2008
Received in revised form 18 December 2008
Accepted 8 January 2009
Available online 14 January 2009

Dedicated to Professor Carlos C. Romão on the occasion of his 60th birthday.

Keywords:
Molybdenum
Cyclopentadienyl ligands
Carbonyl ligands
Amino acids
Epoxidation

ABSTRACT

The complex [(N-benzyloxycarbonylprolyl)cyclopentadienyl]-Mo(CO)$_3$Me was prepared by the reaction of the amino acid-functionalized cyclopentadienyl-lithium reagent with Mo(CO)$_6$, and subsequent methylation with CH$_3$I. The complex was characterized by FTIR, ^{1}H and ^{13}C NMR, and elemental analysis. A single-crystal X-ray diffraction study showed that the complex is chiral, crystallizing in the orthorhombic $P2_12_12_1$ space group with the Flack parameter refining to –0.007(16), which unequivocally confirms the presence of an enantiomerically pure compound. The complex was examined as a catalyst precursor in the liquid-phase epoxidation of *trans*-β-methylstyrene at 280–330 K, using either *tert*-butylhydroperoxide (*tert*-BuOOH), cumylhydroperoxide or urea-hydrogen peroxide adduct as oxidant, and, optionally, a co-solvent. With chloroform and *tert*-BuOOH, the catalytic activity surpasses that previously reported for chiral complexes of the type CpMo(CO)$_3$X, giving the epoxide isomers ((R,R)-(+) and (S,S)-(−)-1-phenylpropylene oxide) in excellent selectivity, albeit with negligible enantiomeric excess. FTIR spectroscopy showed that the oxidative decarbonylation of the tricarbonyl complex with *tert*-BuOOH is fast under the reaction conditions used, and that the structural integrity of the amino acid-functionalized cyclopentadienyl group is retained during this process. The use of the ionic liquid 1-butyl-3-methylimidazolium tetrafluoroborate as a solvent for the catalyst generates a biphasic liquid–liquid reaction system that enables, at the end of a catalytic cycle, the separation and reutilization of the catalyst.

1. Introduction

Recent work has shown that cyclopentadienyl molybdenum tricarbonyl complexes Cp′Mo(CO)$_3$X (Cp′ = η^5-C$_5$R$_5$; X = Cl, alkyl, *ansa*-alkyl) are effective catalyst precursors in liquid-phase olefin epoxidation [1]. In situ oxidation by the oxidant used in the epoxidation, *tert*-butylhydroperoxide, gives rise to the actual Mo^{VI} active species. Although the exact nature of the species formed during in situ oxidation is not yet completely unraveled, products which may be formed are the oxides Cp′MoO$_2$X and [Cp′MoO$_2$]$_2$(μ-O), the peroxo complexes Cp′MoO(O$_2$)X and [Cp′MoO(O$_2$)]$_2$(μ-O), and the anionic trioxo complex [Cp′MoO$_3$]$^-$ [1h].

The successful application of these complexes in epoxidation catalysis led to the development of chiral cyclopentadienyl molybdenum tricarbonyl complexes in an attempt to obtain enantioselective epoxidation catalysts [2]. *Ansa*-bridged complexes with stereogenic centres located in the side chain were synthesized and tested as catalysts for the asymmetric epoxidation of *trans*-β-methylstyrene [2a]. Although chiral inductions of up to *ca.* 20% were observed, the high ring strain of the *ansa*-bridged system led to stability problems under the oxidizing conditions. Parallel to this study, a cyclopentadienyl molybdenum tricarbonyl complex with a chiral menthyl group attached to the cyclopentadienyl ring was synthesized and tested as an enantioselective catalyst [2b]. Although catalytic results regarding enantiomeric excess (ee) were not able to surpass the previous ones, the good catalyst stability enabled the ee to be maintained over the entire catalytic reaction. Thus, the functionalization of the cyclopentadienyl ring with other chiral ligands is a potentially useful strategy for the synthesis of new chiral catalysts of the type Cp′Mo(CO)$_3$X.

Despite the fact that ligand effects are usually determinant for a catalysts′ performance, they are not easily predictable factors, especially in enantioselective catalysis [3]. Therefore, ligand variation and selection by trial and error is still a commonly used strategy. In order to minimize the effort associated with the

* Corresponding author. Tel.: +351 22 508 1618; fax: +351 22 508 1674.
E-mail address: mra@fe.up.pt (M. Abrantes).

0022-328X/$ - see front matter © 2009 Elsevier B.V. All rights reserved.
doi:10.1016/j.jorganchem.2009.01.012

synthesis of many different ligands (in the search of structural variety), a modular ligand design is highly desirable. This offers the possibility of a flexible, divergent (or even combinatorial) generation of a catalyst library, which can then be screened for catalytic activity. Amino acids are considered good chiral modules to build ligands due to their commercial availability, diversity, assembling and modification possibility [3]. Amino acids and peptides, and their synthetic derivatives, have been used as asymmetric catalysts for a variety of reactions both per se [4] and associated with a metal moiety [5], which demonstrates their chiral induction potential. Metal cyclopentadienyl complexes possessing a specific amino acid moiety are already described in the literature [6]. The synthesis of these complexes is usually performed in the context of the development of drug candidates, biological markers and models for the interaction of biomolecules and metal complexes.

The present work aims at combining complexes of the type $Cp'Mo(CO)_3R$ with amino acids with the objective of obtaining new enantioselective epoxidation catalysts.

2. Results and discussion

2.1. Synthesis and characterization

The cyclopentadienyl precursor, (N-benzyloxycarbonylprolyl)cyclopentadienyllithium, was prepared using a slightly modified literature procedure (Scheme 1) [7], which makes use of a commonly used coupling method from peptide chemistry that favors retention of the configuration of the amino acid used, thus rendering an amino acid-functionalized cyclopentadienyl system showing optical activity. These types of acyl cyclopentadienide ligands can be regarded as resonance hybrids of functionalized cyclopentadienyl anion and oxy-anion-substituted pentafulvene descriptions. Crystallographic studies of the related (N,N-dibenzylalanyl)cyclopentadienyllithium product showed that its bonding features correspond to a dominant fulvenolate character (Scheme 1A) with a small contribution of cyclopentadienyl character (Scheme 1B). [(N-benzyloxycarbonylprolyl)cyclopentadienyl]$Mo(CO)_3Me$ (**1**) was prepared by a classical route, in which $Mo(CO)_6$ is refluxed in THF with the corresponding active lithium cyclopentadienyl, thus forming an ionic intermediate, which is then methylated with CH_3I at room temperature (Scheme 1). Compound **1** is a yellow solid that can be exposed to air for brief periods of time but has to be kept under inert atmosphere for long-term storage.

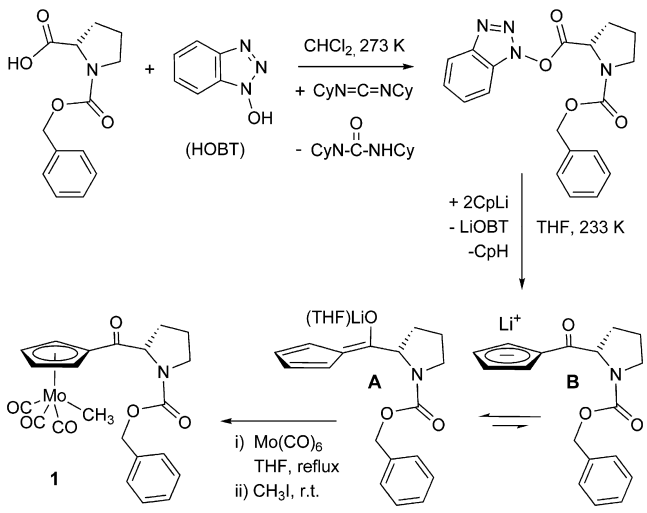

Scheme 1. Synthetic pathway to obtain **1**.

The FTIR spectrum of **1** (KBr pellet) shows three strong metal carbonyl absorptions in the expected range at 2017, 1936 and 1907 cm^{-1}. For comparison, the complex (η^5-C_5H_4COOH)Mo(-$CO)_3Me$ gives rise to three strong absorptions at 2025, 1950 and 1917 cm^{-1} [8]. Complex **1** also shows two strong organic carbonyl absorptions at 1703 and 1683 cm^{-1}, attributed to the ketone and amide functional groups, respectively. The analogous 1,1′-difunctionalized ferrocene complex presents similar bands at 1703 and 1678 cm^{-1} [7].

Details of the NMR investigations are given in the Section 4. In CD_2Cl_2 and at room temperature complex **1** has two well defined sets of NMR signals. This duplication of NMR signals can be explained by an exchange between two rotameric forms [7,9], which, in this case, may arise from a hindered rotation in the N-protected-proline ligand. Acyl prolines, such as N-benzyloxycarbonylproline, are known to suffer from hindered rotation about the N–C bond of the carbamate moiety and are therefore subject to *cis*/*trans*-isomerization [9c]. Under the specified conditions complex **1** exists as a mixture of rotamers in a 50:50 ratio. The resonances of the protons and of the carbon atoms appear in the appropriate range. For each rotamer, the four cyclopentadienyl protons appear as non-equivalent signals corresponding to an ABCD spin system indicating the lack of a symmetry plane in the cyclopentadienyl ring. Accordingly, five resonances were observed in the ^{13}C NMR spectra for the carbon atoms of each rotamer. The proton chemical shifts for both rotamers (5.32–5.85 ppm) are comparable with those for (η^5-C_5H_4COOH)$Mo(CO)_3Me$ (5.68–5.90 ppm) [8].

The crystal structure of **1** was elucidated from single-crystal X-ray diffraction at the low temperature of 150 K (further technical details are given in the Section 4). As expected, the complex is chiral, crystallizing in the orthorhombic $P2_12_12_1$ space group with the Flack parameter [10] refining to –0.007(16), which unequivocally confirms the presence of an enantiomerically pure compound. Fig. 1 shows the thermal ellipsoid plot of the crystallographically independent molecular unit composing this material, and Table 1 lists the bond lengths and angles associated with the molybdenum centre.

The coordination geometry of the crystallographically independent molybdenum centre in **1** strongly resembles a distorted square pyramid: while three carbonyl (C≡O) groups and one

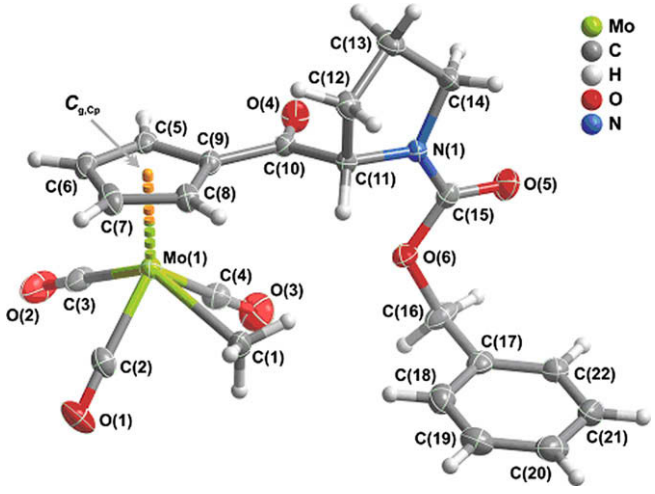

Fig. 1. Schematic representation of the molecular unit present in the crystal structure of [(N-benzyloxycarbonylprolyl)cyclopentadienyl]$Mo(CO)_3Me$ (**1**), showing the labeling scheme for all non-hydrogen atoms. Thermal ellipsoids are drawn at the 30% probability level and hydrogen atoms are represented as small spheres with arbitrary radii. Mo–C bonds to the substituted η^5-Cp organic ligand have been replaced by a dashed bond to the corresponding centre of gravity ($C_{g,Cp}$). For selected bond lengths and angles see Table 1.

methyl group compose the basal plane of the pyramid, the cyclopentadienyl ring of the (N-benzyloxycarbonylprolyl)cyclopentadienyl group occupies the apical position (more clearly observed if all Mo–C bonds are replaced by a single connection to the centre of gravity of the ring, $C_{g,Cp}$ – see Fig. 1). The Cp ring is almost parallel to the average basal plane, with the dihedral angle being 2.7°. Moreover, the metal centre is raised above the basal plane by *ca.* 1.05 Å. Even though searches in the literature and in the Cambridge Structural Database (CSD, Version 5.29 with two updates – August 2008) [11] reveal the existence of a considerable number of tricarbonyl-(substituted-)Cp complexes, those with a coordination geometry resembling that of **1** and having an identical basal plane are much fewer [1b,8,12]. Interestingly, among these related structures only those designed and synthesized by Lai et al. are truly chiral (hence, optically active), and contain either derivatives of (−)-pinane [12e,12h] or carbohydrate-substituted cyclopentadienes [12b,12f].

The distinct nature of the chemical moieties composing the molybdenum first coordination sphere are markedly reflected in the registered bond lengths (Table 1): while the Mo–C for the C≡O groups range from 1.9732(19) to 1.9962(19) Å, and the Mo–CH_3 bond length is 2.3148(17) Å, the Mo–C distances for the substituted Cp ring are instead found in the 2.3160(16)–2.3922(18) Å range (with the Mo···$C_{g,Cp}$ distance being *ca.* 2.02 Å). Most of the bond lengths in **1** are comparable with those for related molybdenum complexes, as revealed by systematic searches in the CSD for geometrical data on similar structural arrangements: for Mo–$(C{\equiv}O)_3$, the Mo–C distances are usually found in the range of 1.57–2.35 Å, with a median of 2.02 Å (among 1619 hits in the CSD); the Mo–C distances with Cp rings (search limited to tricarbonyl complexes) are usually in the range of 2.25–2.55 Å (median of 2.34 Å; 338 hits in the database), with these values also fully supporting the assumption of a typical η^5-coordination mode for the Cp ring in **1**. However, while the common Mo–CH_3 interactions have a median bond distance of only *ca.* 2.21 Å (29 hits; 2.03–2.42 Å range), the corresponding bond in **1** is considerably longer. Nevertheless, a close inspection of all known structures with longer Mo–CH_3 interactions (i.e., in the upper 2.30–2.42 Å quartile) reveals that this is indeed a common feature among tricarbonyl complexes [12a–j,12m]. The observed bond angles for the coordination polyhedron further support the presence of a distorted square pyramid: while the angles with the apical position ($C_{g,Cp}$) range from 111.37(1)° to 128.60(1)°, those within the basal plane and between neighboring ligands (*cis*-connections) vary between 71.12(8)° and 79.54(8)° (Table 1).

The close packing of [(N-benzyloxycarbonylprolyl)cyclopentadienyl]Mo$(CO)_3$Me molecular units in the solid state is essentially mediated by weak interactions (offset π–π stacking and some weak C–H···O hydrogen bonds) and the need to effectively fill the available space (Fig. 2). For example, some C≡O groups interact with neighboring moieties via weak C–H···O contacts (not shown), with the *d*(O···C) internuclear distances and <(OHC) angles varying between 3.31–3.38 Å and 119–146°. However, these interactions seem to be of a very weak nature since they do not induce any deviation from linearity in the refined <(Mo–C≡O) angles [found in the 176.92(19)–178.72(16)° range]. The most prominent supramolecular contacts in **1** concern the offset π-π stacking between the substituted Cp rings and the terminal benzyl groups of the (N-benzyloxycarbonylprolyl)cyclopentadienyl ligand belonging to a neighboring complex. Indeed, even though the Cp ring subtends a tilt angle of *ca.* 6.7° with respect to the adjacent benzyl group, the corresponding centroid is at *ca.* 3.62 Å from the average plane containing the same benzyl moiety, which corresponds to a moderate π-π interaction. This arrangement leads to the formation of a supramolecular tape along the [0 1 0] direction of the unit cell as represented in Fig. 2.

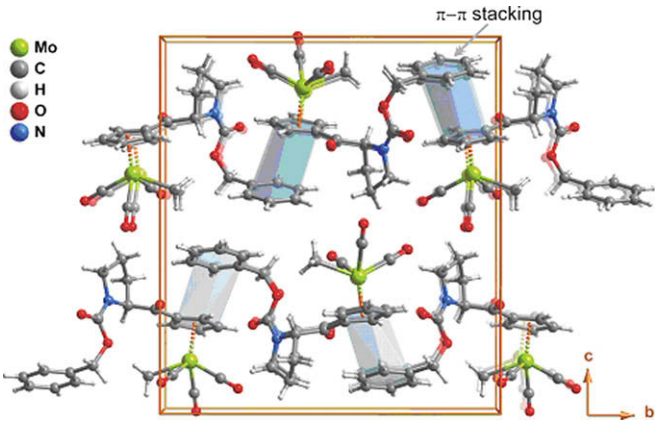

Fig. 2. Crystal packing of [(N-benzyloxycarbonylprolyl)cyclopentadienyl]Mo$(CO)_3$-Me (**1**) viewed in perspective along the [1 0 0] crystallographic direction. Mo–C bonds to the substituted Cp ring have been replaced by a dashed bond to the corresponding centre of gravity ($C_{g,Cp}$). Offset π–π stacking interactions connecting adjacent molecular units and leading to the formation of a supramolecular tape parallel to the *b*-axis are represented as blue-filled polygons.

Table 1
Selected bond lengths (Å) and angles (°) for the molybdenum coordination environment present in [(N-benzyloxycarbonylprolyl)cyclopentadienyl]Mo$(CO)_3$Me (**1**).[a]

Mo(1)–C(1)	2.3148(17)	$C_{g,Cp}$–Mo(1)–C(1)	111.37(1)
Mo(1)–C(2)	1.9906(19)	$C_{g,Cp}$–Mo(1)–C(2)	128.60(1)
Mo(1)–C(3)	1.9962(19)	$C_{g,Cp}$–Mo(1)–C(3)	116.51(1)
Mo(1)–C(4)	1.9732(19)	$C_{g,Cp}$–Mo(1)–C(4)	128.30(1)
Mo(1)–C(5)	2.3160(16)	C(1)–Mo(1)–C(2)	72.37(7)
Mo(1)–C(6)	2.3510(17)	C(1)–Mo(1)–C(3)	132.13(7)
Mo(1)–C(7)	2.3922(18)	C(1)–Mo(1)–C(4)	71.12(8)
Mo(1)–C(8)	2.3718(17)	C(2)–Mo(1)–C(3)	78.07(8)
Mo(1)–C(9)	2.3213(16)	C(2)–Mo(1)–C(4)	102.08(8)
Mo(1)···$C_{g,Cp}$	2.0162(1)	C(3)–Mo(1)–C(4)	79.54(8)

[a] $C_{g,Cp}$ – centroid of the coordinated η^5-Cp-substituted aromatic rings [C(5)–C(9)].

2.2. Catalytic olefin epoxidation

2.2.1. Preliminary screening and effect of temperature

The catalytic performance of **1** for the epoxidation of *trans*-β-methylstyrene, chosen as a model substrate for an unfunctionalized prochiral *trans*-olefin, was explored using 5.5 M *tert*-butylhydroperoxide (*tert*-BuOOH) in decane as oxidant and chloroform as co-solvent (Scheme 2). The interest in studying *trans*-olefins as substrates arises from the fact that the existing Mn/salen (Jacobsen-Katsuki) system for non-functionalized olefins works efficiently for terminal and *cis*-substituted olefins but less efficiently for *trans*-olefins [13].

In the temperature range 300–330 K and during the first 4 h of reaction in the presence of compound **1**, the corresponding epoxide isomers ((*R,R*)-(+) and (*S,S*)-(−)-1-(phenylpropylene oxide)) are formed with excellent selectivity (>98%, at 77–96% conversion) (Table 2). However, enantiomeric excess (ee) is negligible (<5%) under the reaction conditions used. Since lower temperatures are

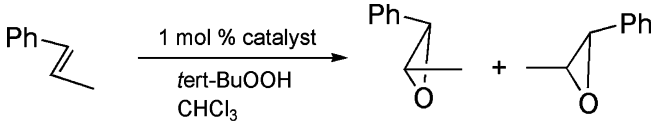

Scheme 2. Catalytic epoxidation of *trans*-β-methylstyrene in the presence of **1**.

Table 2
Catalytic results of *trans*-β-methylstyrene epoxidation in the presence of **1** or **2** using *tert*-BuOOH as oxidant in chloroform.

Catalyst	Temperature (K)	TOF[a] (mol mol_{Mo}^{-1} h^{-1})	Conversion at 4/24 h (%)	Selectivity[b] at 4/24 h (%)
1	330	1106	96/100	99/84
	300	461	77/78	99/84
	280	163	51/–	100/–
2	300	212	49/64	92/85

[a] Turnover frequency calculated at 5 min of reaction.
[b] Selectivity to (*R*,*R*)-(+) and (*S*,*S*)-(−)-1-phenylpropylene oxide; ee was always less than 5%.

usually regarded as beneficial for the improvement of enantioselectivity [2a], attempts to enhance ee by decreasing the reaction temperature to 280 K were made, but no improvement in enantioselectivity was observed and, as could be expected, the reaction rate decreased significantly. Nevertheless, the catalytic activity of **1** surpasses that previously reported for chiral complexes of the type $CpMo(CO)_3X$ that have been tested in the same reaction, at 328 K. For example, after 4 h of reaction, [(−)-menthylCp]-$Mo(CO)_3Cl$ gave a conversion of 34% [2b], and the *ansa* complexes (*S*)-[(η^5-C_5H_4CHPh-η^1-CH_2)$Mo(CO)_3$] and (*R*,*S*)-[(η^5-C_5H_4CHMe-η^1-CHMe)$Mo(CO)_3$] gave conversions of 66% and 50%, respectively [2a]; the overall selectivity to epoxides was always 100% and ee was 5–20% [2]. At room temperature, the *ansa* complexes gave less than 20% epoxide yield after 24 h [2a].

No induction periods were detected even at low temperatures, indicating that active oxidizing species are formed within the first few minutes of reaction, possibly in large amounts if poorly active, or in small amounts if fairly active. The kinetic profiles reveal that the reaction rate tends to decrease with time (Fig. 3). Previous mechanistic studies involving pseudo-octahedral dioxomolybdenum(VI) complexes bearing organic Lewis base ligands (MoO_2L_n, *n* represents the number of neutral/charged ligands, such as halide, alkyl, Lewis base) have indicated *tert*-butanol as a possible inhibitor in the epoxidation reaction due to its coordinating ability [14]. One could expect a similar inhibitory effect for complex **1**, since it may be oxidized into, among other species, dioxomolybdenum(VI) active species (as discussed ahead), which may react further with the oxidant to give the active oxidizing species for the oxygen atom transfer to the olefin.

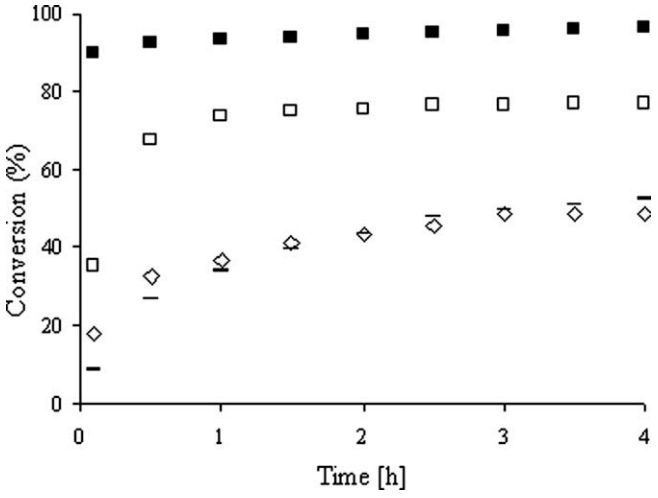

Fig. 3. Kinetic profiles of the reaction of *trans*-β-methylstyrene with *tert*-BuOOH in the presence of **1** or **2**, using $CHCl_3$ as solvent: ■ (**1** at 330 K), □ (**1** at 300 K), – (**1** at 280 K) and ◇ (**2** at 300 K).

No reaction occurs in the presence of **1** without *tert*-BuOOH, indicating that the oxidant is required for generating the active oxidizing species, which may be a *tert*-butylperoxo-molybdenum intermediate, as proposed for MoO_2L_n complexes [1c]. The decrease in reaction rate with time may also result from a relatively short lifetime of the catalyst: for example, at 300 K, conversions at 4 h and 24 h are similar and epoxide selectivity decreases with time (*ca.* 78%, Table 2). The fact that the time required to reach a plateau for olefin conversion increases as the temperature decreases (Fig. 3) suggests that catalyst deactivation is involved.

2.2.2. Study of the oxidation of 1 with tert-BuOOH

In order to get some insight into the oxidative transformation of complex **1** in the presence of *tert*-BuOOH, the reaction was followed by FTIR spectroscopy at 293 K. Complex **1** was dissolved in chloroform and *tert*-BuOOH was added in the same proportion as used in the catalytic tests (catalyst:oxidant molar ratio = 1:200). Whereas in the solid state spectrum (KBr pellet) three carbonyl absorption bands are well distinguished for complex **1**, in chloroform solution (prior to the addition of *tert*-BuOOH) the two low-frequency bands overlap such that only one broad, asymmetric peak is observed, centred around 1939 cm^{-1} (Fig. 4). The other band is found at 2029 cm^{-1} and therefore shifted to higher frequency by about 10 cm^{-1} compared with the corresponding band in the solid state spectrum. The two organic CO absorptions at 1703 and 1683 cm^{-1} in the KBr pellet spectrum are shifted by 9 cm^{-1} to higher frequency in the $CHCl_3$ spectrum, and are less clearly resolved. These differences may be attributed to solvation effects due to the exchange between rotameric forms in solution, in agreement with the NMR data discussed above. As expected, no peaks characteristic of Mo=O vibrations were observed in the FTIR spectrum of **1** in $CHCl_3$, indicating that the complex is relatively stable towards oxidation under air.

After addition of *tert*-BuOOH to **1** in $CHCl_3$, the bands assigned to the carbonyl ligands start to decrease in intensity and after 2 h they become residual (Fig. 5, bands a and b). These results suggest that the oxidative decarbonylation of **1** is nearly complete within 2 h. As mentioned above, the reaction of the olefin at 300 K reaches nearly maximum conversion (76%) within this period of time, with no relevant induction period. These results suggest that the active species formed within the first few minutes are fairly active in the olefin epoxidation. However, as suggested above, these species may undergo consecutive chemical transformations into less active or inactive species, thereby affecting the reaction rate.

While it is clear that the oxidizing medium leads to the displacement of the CO ligands, it does not seem to have a significant effect on the (N-benzyloxycarbonylprolyl)cyclopentadienyl ligand.

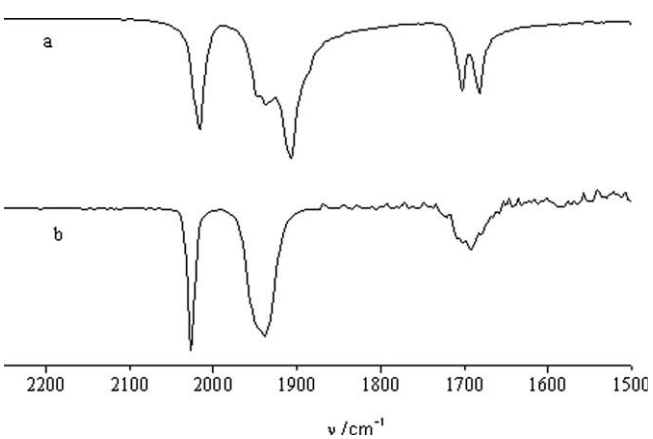

Fig. 4. FTIR spectra of compound **1** in KBr (a) and $CHCl_3$ (b).

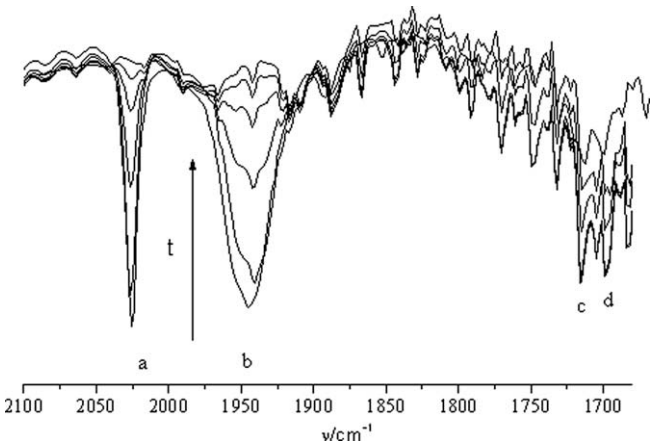

Fig. 5. Oxidation of **1** in $CHCl_3$ with *tert*-BuOOH followed by FTIR. Following the direction of the time arrow: 0 min (prior to addition of the oxidant), and 5, 30, 60, 120 and 240 min after addition of *tert*-BuOOH. Metal carbonyl bands are indicated by a and b, and organic carbonyl bands are indicated by c and d.

Thus, despite the irregularity of the baseline, it is evident that the bands arising from the organic carbonyl groups persist throughout the oxidation process (Fig. 5, bands c and d), albeit with some changes in the relative intensities and broadening to contiguous vibrations. If the ligand suffered decomposition one would expect its signals to decrease significantly or even disappear, which is not the case. Accordingly, and taking into account the mechanistic assumptions outlined above, the lack of chiral induction ability of the active species is probably due to free rotation of the cyclopentadienyl and/or amino acid groups, imposing minor stereochemical constraints with the interacting olefin. As mentioned in the introduction, a mixture of different oxomolybdenum species (dioxo, oxoperoxo, mono/dimeric) may be formed during the oxidation process (see the discussion below for the recovered solid **2**). Unfortunately, information regarding the appearance of Mo–O stretching vibrations cannot be obtained since *tert*-butanol, the by-product of *tert*-BuOOH, presents a strong absorption band in the same region of the IR spectrum, and since its concentration varies during the reaction the subtraction of the spectrum of *tert*-BuOH does not give reliable results.

Attempts were made to isolate the metal complex(es) after catalysis for characterization studies. After 4 h of reaction of the olefin, a solid was isolated. No quenching with MnO_2 was performed since this could destroy and/or modify the catalytically active species. The volatiles were carefully evaporated at room temperature and the resulting yellow residue was washed thoroughly with pentane to give **2**. The solid was characterized by FTIR, ^{1}H NMR and elemental analysis, but the likely presence of a mixture of species prevented their unambiguous identification. Nevertheless, the FTIR spectrum of **2** (KBr pellet) showed no bands assigned to metal carbonyl vibrations, and displayed bands at 1684 and 1696 cm^{-1} for the organic carbonyl groups. The shift in the latter bands compared with those for **1** may be due to changes in the coordination sphere of the metal. ^{1}H NMR confirmed the presence of the phenyl group of the amino acid moiety (multiplet in the range 7.25–7.44 ppm).

The reaction with the olefin was carried out in the presence of **2** at 300 K, using $CHCl_3$ as solvent. No reaction occurs in the absence of *tert*-BuOOH, while in the presence of oxidant the reaction takes place without an initial induction period, as found for **1** (Fig. 3). The reaction of the olefin in the presence of **2** is slower than that observed for **1**. The solid **2** originates mainly the corresponding epoxide isomers (ee is negligible), and the total epoxides selectivity is somewhat lower than that observed for **1** (Table 2). As mentioned above, the recovered solid probably consists of a mixture of different metal species possessing different catalytic properties. The fact that the recovered solid **2** possesses catalytic activity suggests that catalyst decomposition is not complete (at least after 4 h) and that it is not solely responsible for the decrease in reaction rate with time.

2.2.3. Solvent effects

Experiments to assess the influence of the solvent on the catalytic performance of **1** were carried at 300 K, using aprotic solvents (chloroform, dichloromethane, toluene and without co-solvent) and a protic solvent (methanol). Since all these solvents appear to give homogeneous catalytic systems, the influence of the solubility of the metal species on the catalytic performance can be neglected (Table 3, Fig. 6). The ee was always less than 5%. The aprotic solvents give relatively high total epoxides selectivity throughout 24 h (82–98%). In contrast, methanol gives very low epoxide yield at 24 h (<1%) due to the very slow reaction and the low selectivity to epoxides.

After the first 5 min of reaction, conversion follows the order: no co-solvent ≅ chloroform > toluene > dichloromethane > methanol. The fact that the highest TOF occurs when no co-solvent is used is probably due, at least in part, to the higher catalyst and

Table 3
Catalytic results of *trans*-β-methylstyrene epoxidation in the presence of **1** at 300 K.

Solvent	Oxidant	TOF[a] (mol mol_{Mo}^{-1} h^{-1})	Conversion[b] (%)	Selectivity[c] (%)
$CHCl_3$	*tert*-BuOOH	461	78/78	98/92
None	*tert*-BuOOH	561	76/81	91/88
CH_2Cl_2	*tert*-BuOOH	270	44/49	88/82
Toluene	*tert*-BuOOH	318	63/71	96/91
Methanol	*tert*-BuOOH	43	8/11	4/3
$[BMIM]BF_4$	*tert*-BuOOH	423	41/47	19/20
		–	32/43[d]	12/12[d]
$CHCl_3$	cumylOOH	36	15/29	99/73
$CHCl_3$	UHP	0	<3/<3	5/10

[a] Turnover frequency calculated at 5 min of reaction.
[b] Conversion at 4/24 h.
[c] Selectivity at 4/24 h to (*R*,*R*)-(+) and (*S*,*S*)-(−)-1-phenylpropylene oxide; ee was always less than 5%.
[d] Second batch.

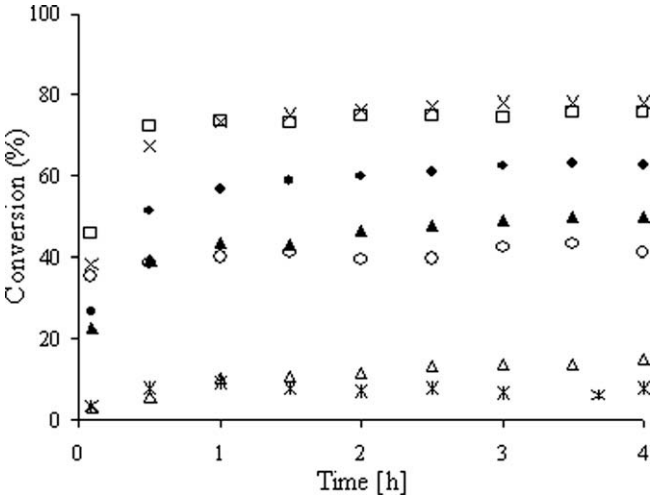

Fig. 6. Kinetic profiles of the reaction of *trans*-β-methylstyrene in the presence of compound **1** at 300 K: □ (without solvent, *tert*-BuOOH), × (chloroform, *tert*-BuOOH), ● (toluene, *tert*-BuOOH), ▲ (dichloromethane, *tert*-BuOOH), ○ ($[BMIM]BF_4$, *tert*-BuOOH), ∗ (methanol, *tert*-BuOOH) and Δ (chloroform, cumyl hydroperoxide).

oxidant concentrations. The sluggish reaction observed in methanol may likely be caused by solvent competition with the oxidant for coordination to the metal centre, as already proposed for the *tert*-butanol formed during the catalytic reaction [1h]. For all solvents studied and without co-solvent, conversions at 4 h and 24 h are similar.

The reaction of *trans*-β-methylstyrene with *tert*-BuOOH was also carried out using complex **1** dissolved in the ionic liquid (IL) [BMIM]BF_4 (BMIM = 1-butyl-3-methylimidazolium) at 300 K. Under these conditions, the catalyst is completely soluble in the IL, which can be considered as a "liquid support" that facilitates the reuse of the catalyst and may even enhance its stability. This IL has been used to enhance enantioselectivity in hydrogenation reactions performed with ruthenium catalysts [15]. After complete dissolution of **1** in the IL, the addition of the olefin and oxidant resulted in a biphasic liquid–liquid reaction system. The upper phase remained colorless during the reaction, while the IL phase was yellow, suggesting that the metal species were essentially dissolved in the latter. Unfortunately, no improvement in ee was observed by performing the epoxidation reaction in [BMIM]BF_4. Epoxide yield between 4 and 24 h (7–10%) was lower than that observed for the aprotic solvents (38–77%), and higher than that obtained using methanol (<1%). Possibly, the active species formed in the IL are different from those formed in the organic solvents. After removing the upper phase and recharging the reaction vessel with more substrate and oxidant, it was possible to reuse the IL phase containing the catalyst in a second batch, although both the conversion and epoxide selectivity decreased compared with the values in the first batch (Table 3).

2.2.4. Effect of oxidant

Experiments to assess the influence of the oxidant on the catalytic performance were carried out at 300 K using *tert*-BuOOH in decane, cumylhydroperoxide (cumylOOH) or urea-hydrogen peroxide adduct (UHP), and chloroform as solvent. UHP was used as a source of "dry" hydrogen peroxide, since water is thought to have a detrimental effect on the activity of related molybdenum complexes [1d]. The catalytic systems with the organic hydroperoxides are homogeneous, while UHP is not completely soluble in the reaction medium. As shown in Table 3 and Fig. 6, the reaction rate is much higher for *tert*-BuOOH than for cumylOOH, and is negligible for UHP (<3% conversion at 24 h). The sluggish reaction in the presence of UHP could be due to the limited solubility and/or the slow dissociation of UHP in the reaction medium, as well as the limited ability of the metal species to activate H_2O_2. A considerable amount of peroxide in the reaction medium was detected using test sticks for semiquantitative determination of peroxides. Hence, the poor catalytic results observed for UHP are better explained by the limited ability of **1** to activate H_2O_2, as reported previously for $CpMo(CO)_3Cl$ [1h]. It is worth noting, however, that $Cp'Mo(CO)_3Cl$ complexes were recently reported to be catalytically efficient in the oxidation of sulfides with aqueous H_2O_2 [16]. The poor catalytic performance observed when cumylOOH is the oxidant may be due to steric (the cumyl group is bulkier than the *tert*-butyl group) and/or electronic effects (the basicity of cumylOOH is possibly weaker than that of *tert*-BuOOH). These factors may be partially responsible for a slower oxidative decarbonylation step and/or a slower formation of the intermediate active oxidizing species. Furthermore, like *tert*-butanol, the by-product cumyl alcohol may act as a competitive inhibitor.

3. Conclusions

An amino acid-functionalized cyclopentadienyl molybdenum tricarbonyl complex, [(N-benzyloxycarbonylprolyl)cyclopentadienyl]$Mo(CO)_3Me$, was successfully synthesized using a combination of organometallic and peptide chemistry. NMR spectroscopic investigations indicate that two rotameric forms of the complex are present in solution. A single-crystal X-ray diffraction study showed that the complex is chiral, crystallizing in the orthorhombic $P2_12_12_1$ space group with the Flack parameter refining to −0.007(16), which unequivocally confirms the presence of an enantiomerically pure compound. The complex can be used as a catalyst precursor for the epoxidation of *trans*-β-methylstyrene. Although the enantiomeric excess is negligible under all conditions studied, results regarding conversion clearly surpass those previously obtained for chiral complexes of this type that have been tested under similar reaction conditions. The complex preferentially activates organic peroxides for the catalytic reaction. Using *tert*-BuOOH as oxidant, aprotic solvents lead to a high selectivity to epoxides. The use of the ionic liquid [BMIM]BF_4 generates a biphasic liquid–liquid reaction system that allows, at the end of a catalytic cycle, the separation and reuse of the catalyst. Studies regarding the metal species resulting from the oxidation of the cyclopentadienyl molybdenum tricarbonyl precursor show that the amino acid moiety linked to the cyclopentadienyl ring retains its integrity. The solid isolated after a catalytic run is also active as a catalyst for the epoxidation of *trans*-β-methylstyrene in the presence of *tert*-BuOOH with selectivities similar to the carbonyl complex. In the future, attempts to separate the metal species by preparative chromatography will be made, which should facilitate their characterization.

4. Experimental

4.1. General methods and procedures

4.1.1. Characterization

Microanalyses were performed at the Laboratory of Catalysis and Materials, Faculty of Engineering, University of Porto. IR spectra were obtained by the KBr pellet method using a FTIR Mattson-7000 infrared spectrophotometer. ^1H, $^{13}C\{^1H\}$, ^{13}C, ^1H HMQC and JMOD NMR experiments were performed at the University of Cambridge (Department of Chemistry) using a BRUKER Avance 500 Cryo Ultrashield spectrometer (^1H, 500 MHz; ^{13}C, 126 MHz). Chemical shifts are quoted in parts per million from tetramethylsilane.

4.1.2. Syntheses

Unless otherwise stated all preparations and manipulations were carried out using Schlenk techniques under nitrogen. Solvents were dried by standard procedures (*n*-hexane, diethyl ether and THF with Na/benzophenone ketyl; dichloromethane with CaH_2), distilled under nitrogen and used immediately (for THF) or kept over 4 Å molecular sieves. Cyclopentadienyllithium (CpLi) was synthesized as described previously [17]. N-benzyloxycarbonyl-l-proline was purchased from Panreac and hydroxybenzotriazole (HOBT), dicyclohexylcarbodiimide (DCC), urea hydrogen peroxide (UHP) and 1-butyl-3-methylimidazolium tetrafluoroborate ([BMIM]BF_4) from Fluka.

4.2. (N-benzyloxycarbonylprolyl)cyclopentadienyllithium

A solution of DCC (1.74 g, 8.4 mmol) in CH_2Cl_2 (25 mL) was added under air to a suspension of N-benzyloxycarbonyl-l-proline (2.10 g, 8.4 mmol) and HOBT (1.14 g, 8.4 mmol) in CH_2Cl_2 (25 mL) at 273 K. After stirring for 1 h at 273 K the precipitated N,N′-dicyclohexylurea was filtered off and the filtrate was evaporated to dryness giving the active ester as a white sticky compound. In a Schlenk tube a suspension of the active ester in dry THF (30 mL) was cooled to 233 K and a solution of CpLi (1.22 g, 17 mmol) in

dry THF (40 mL) cooled to 233 K was added. The yellow solution was allowed to warm up to room temperature overnight, ultimately becoming a suspension. The solvent was removed in vacuo and the resultant residue extracted with dry diethyl ether (3 × 30 mL) to separate the desired reaction product from LiOBT and any excess CpLi. A brown solid was obtained after concentration of the diethyl ether extract to dryness in vacuo. Yield: 1.93 g, 61%.

4.3. [(N-benzyloxycarbonylprolyl)cyclopentadienyl]Mo(CO)$_3$Me (**1**)

$Mo(CO)_6$ (0.6 g, 2.3 mmol), (N-benzyloxycarbonylprolyl)cyclopentadienyl-lithium (0.85 g, 2.3 mmol) and dry THF (50 mL) were added to a Schlenk tube under inert atmosphere and refluxed for 20 h. A brown solution was obtained, which was cooled down to room temperature. CH_3I (4 mL, 6.4 mmol) was added and, after stirring for 5 h, the solvent was removed in vacuo to give a yellowish brown residue. This residue was purified by column chromatography under air using silica gel as stationary phase. The target compound was eluted with a mixture of hexane:CH_2Cl_2 (10:1) with 1% of NEt_3. The orange oil obtained was further purified by recrystallization (CH_2Cl_2/hexane) and washing with pentane. A yellow solid was isolated. Yield: 0.67 g, 60%. $C_{22}H_{21}MoNO_6$ (491.35): Calc.: C, 53.78; H, 4.31; N, 2.85. Found: C, 53.40; H, 4.50; N, 2.90%. FTIR (KBr): nu(tilde) = 3089 (w), 2985 (w), 2954 (w), 2931 (w), 2886 (w), 2017 (vs, ν_{Mo-CO}), 1936 (vs, ν_{Mo-CO}), 1907 (vs, ν_{Mo-CO}), 1702 (s, ν_{CO}, ketone), 1681 (s, ν_{CO}, amide), 1463 (m), 1421 (m), 1380 (w), 1340 (m), 1309 (w), 1249 (m), 1207 (w), 1180 (w), 1126 (m), 1089 (w), 1060 (w), 909 (w), 889 (w), 852 (w), 765 (w), 738 (w), 698 (w), 588 (w), 563 (w), 505 (w), 478 (w) cm^{-1}. ^1H NMR (500 MHz, CD_2Cl_2, 298 K): δ 7.37–7.24 (complex signal, 2 × 5H, Ph), 5.85 (m, 1H, Cp-α), 5.71 (m, 1H, Cp-α,), 5.68 (m, 1H, Cp-α), 5.63 (m, 1H, Cp-α), 5.49 (m, 1H, Cp-β), 5.44 (m, 1H, Cp-β), 5.36 (m, 1H, Cp-β), 5.32 (m, 1H, Cp-β), 5.13 (d, J = 13.0 Hz, 1H, CH_2-Ph), 5.10 (d, J = 12.5 Hz, 1H, CH_2-Ph), 5.08 (d, J = 12.5 Hz, 1H, CH'_2-Ph), 4.98 (d, J = 12.5 Hz, 1H, CH'_2-Ph), 4.69 (dd, J = 8.5 Hz, J = 4.0 Hz, 1H, N-CH), 4.66 (dd, J = 9.5 Hz, J = 4.5 Hz, 1H, N-CH'), 3.56 (m, 2 × 2H, $^{14}CH_2$), 2.32 (m, 2 × 1H, $^{12}CH_2$), 2.00 (m, 2 × 1H, $^{12}CH_2$), 1.93 (m, 2 × 2H, $^{13}CH_2$), 0.48 (s, 3H, -CH_3), 0.43 (s, 3H, -CH_3) ppm. ^{13}C {^1H} NMR (126 MHz, CD_2Cl_2, 298 K): δ 237.2, 237.1 (CO *trans* to CH_3, C^3), 224.9, 224.8, 224.7 (CO *cis* to CH_3, C^2, C^4), 196.0, 195.8 (C^{10}), 154.7, 154.4 (C^{15}), 136.9, 136.8 (C^{17}), 128.6, 128.5, 128.4, 128.3, 128.1, 128.0, 127.9 (C^{18}–C^{22}), 102.4, 101.7 (C^9), 97.0, 96.7, 96.6 (Cp-β, C^6 and C^7), 93.4, 93.3, 93.1, 92.6 (Cp-α, C^5 and C^8), 67.1, 67.0 (C^{16}), 62.1, 62.0 (C^{11}), 47.5, 46.9 (C^{14}), 32.4, 31.2 (C^{12}), 24.9, 23.8 (C^{13}), −19.6 CH_3, C^1) ppm. JMOD (J-Modulated spin-echo experiment) (126 MHz, CD_2Cl_2, 298 K): Quaternary and methylene C: δ 237.2, 237.1 (CO *trans* to CH_3, C^3), 224.9, 224.8, 224.8, 224.7 (CO *cis* to CH_3, C^2 and C^4), 196.0, 195.8 (C^{10}), 154.8, 154.3 (C^{15}), 137.3, 137.2 (C^{17}), 102.4, 101.7 (C^9), 67.1, (C^{16}), 47.5, 46.9 (C^{14}), 32.4, 31.2 (C^{12}), 24.9, 23.8 (C^{13}) ppm. Methyne and methyl C: δ 128.6, 128.5, 128.4, 128.3, 128.1, 128.0, 127.9 (C^{18}–C^{22}), 97.0, 96.7, 96.6 (Cp-β, C^6–C^7), 93.4, 93.3, 93.1, 92.6 (Cp-α, C^5, C^8), 62.1, 61.8 (C^{11}), −19.6 (C^1) ppm. ^{13}C, ^1H HMQC (126/500 MHz, CD_2Cl_2, 298 K): δ ^{13}C/δ ^1H = 128.6, 128.5, 128.4, 128.3, 128.1, 128.0, 127.9/7.37–7.24 (Ph), 97.0, 96.7, 96.6/5.49, 5.44, 5.36, 5.32 (Cp-β), 93.4, 93.3, 93.1, 92.6/5.85, 5.71, 5.68, 5.63 (Cp-α), 67.1, 67.0/5.13, 5.10 (CH_2-Ph), 5.08, 4.98 (CH'_2-Ph), 62.1, 62.0/4.69, 4.66 (C^{11}/H^{11}), 47.5, 46.9/3.56 (C^{14}/H^{14}), 32.3, 31.2/2.32, 2.00 (C^{12}/H^{12}), 24.9, 23.8/1.93 (C^{13}/H^{13}), −19.6/0.48, 0.43 (CH_3) ppm (see Fig. 1 for atom numbering).

4.4. Single-crystal X-ray diffraction studies

Yellow single-crystals of [(N-benzyloxycarbonylprolyl)-cyclopentadienyl]Mo(CO)$_3$Me (**1**), kept under a nitrogen atmosphere, were immediately covered by FOMBLIN Y perfluoropolyether vacuum oil (LVAC 25/6) purchased from Aldrich [18] after the destruction of the glass seal in order to avoid decomposition. A suitable single-crystal was mounted on a Hampton Research CryoLoop with the help of a Stemi 2000 stereomicroscope equipped with Carl Zeiss lenses. Data were collected at 150(2) K on a Bruker X8 Kappa APEX II CCD area-detector diffractometer (Mo Kα graphite-monochromated radiation, λ = 0.71073 Å) controlled by the APEX2 software package [19], and equipped with an Oxford Cryosystems Series 700 cryostream monitored remotely using the software interface CRYOPAD [20]. Images were processed using the software package SAINT+ [21], and data were corrected for absorption by the multi-scan semi-empirical method implemented in SADABS [22]. The structure was solved in the non-centrosymmetric $P2_12_12_1$ space group (as indicated by the systematic absences inspected using the XPREP interface) by employing the Patterson synthesis algorithm implemented in SHELXS-97 [23,24]. This strategy allowed the immediate location of the molybdenum centre with all remaining non-hydrogen atoms being located from difference Fourier maps calculated from successive full-matrix least squares refinement cycles on F^2 using SHELXL-97 [23,25]. All non-hydrogen atoms were successfully refined using anisotropic displacement parameters. The Flack parameter [10] refined to about –0.007(16) and a total of 3445 Friedel pairs have been merged and were not used as independent data.

Hydrogen atoms bound to carbon were located at their idealized positions using appropriate *HFIX* instructions in SHELXL (43 for the aromatic, 23 for –CH_2–, 13 for the –CH– moieties and 137 for the coordinated methyl group) and included in subsequent refinement cycles in riding-motion approximation with isotropic thermal displacements parameters (U_{iso}) fixed at 1.2 (for the former families of hydrogen atoms) or 1.5 (for the coordinated CH_3 moiety) times U_{eq} of the carbon atom to which they are attached. The last difference Fourier map synthesis showed the highest peak (0.516 e Å^{-3}) and deepest hole (–0.377 e Å^{-3}) located at 0.72 Å from Mo(1) and 1.28 Å from C(18), respectively.

Table 4
Crystal and structure refinement data for [(N-benzyloxycarbonylprolyl)cyclopentadienyl]Mo(CO)$_3$Me (**1**).

Formula	$C_{22}H_{21}MoNO_6$
Formula weight	491.34
Crystal system	Orthorhombic
Space group	$P2_12_12_1$
a (Å)	6.3539(3)
b (Å)	17.1202(9)
c (Å)	19.0463(10)
Volume (Å^3)	2071.86(18)
Z	4
D_{calc} (g cm^{-3})	1.575
μ(Mo Kα) (mm^{-1})	0.672
Crystal size (mm)	0.20 × 0.17 × 0.14
Crystal type	Yellow blocks
θ Range	3.58 to 33.14
Index ranges	$-8 \leqslant h \leqslant 9$ $-25 \leqslant k \leqslant 26$ $-29 \leqslant l \leqslant 29$
Reflections collected	30782
Independent reflections	4442 (R_{int} = 0.0262)
Completeness to θ = 33.14°	99.8%
Final R indices [$I > 2\sigma(I)$][a,b]	R_1 = 0.0209 wR_2 = 0.0507
Final R indices (all data)[a,b]	R_1 = 0.0234 $wR2$ = 0.0516
Weighting scheme[c]	m = 0.0315 n = 0.1075
Largest difference in peak and hole	0.516 and −0.377 e Å^{-3}

[a] $R_1 = \sum||F_o| - |F_c||/\sum|F_o|$.

[b] $wR_2 = \sqrt{\sum[w(F_o^2 - F_c^2)^2]/\sum[w(F_o^2)^2]}$.

[c] $w = 1/[\sigma^2(F_o^2) + (mP)^2 + nP]$ where $P = (F_o^2 + 2F_c^2)/3$.

Information concerning crystallographic data collection and structure refinement details is summarized in Table 4.

4.5. Catalytic olefin epoxidation

The catalytic oxidation of *trans*-β-methylstyrene was carried out at 270, 300 and 330 K under N_2 atmosphere in a reaction vessel equipped with a magnetic stirrer and a condenser. A catalyst:olefin:oxidant molar ratio of 1:100:200 was used. Specifically, the vessel was loaded with *trans*-β-methylstyrene (200 mg, 1.7 mmol), undecane (200 mg, internal standard), 1 mol% of catalyst (8.35 mg, 0.017 mmol), solvent (3 mL) and oxidant (3.4 mmol). The beginning of the reaction is defined as the moment that the oxidant was added. The course of the reaction was monitored by quantitative GC-analysis. Samples were taken every 30 min during the first hours of reaction, diluted with dichloromethane, and a catalytic amount of manganese dioxide added for the destruction of hydroperoxide. The resultant slurry was filtered using a Pasteur pipette fitted with a filter and the filtrate injected in the GC column. The conversion of the olefin as well as the formation of epoxides was quantified by GC using calibration curves recorded prior to the reaction under study.

4.6. Study of the oxidation in the presence of tert-BuOOH

Complex **1** (2.74 mg, 5.6×10^{-3} mmol) was dissolved in $CHCl_3$ (5 mL) under N_2 atmosphere at room temperature (293 K). A sample was taken ($t < 0$). After addition of 5.5 M *tert*-BuOOH in decane (0.2 mL, 1.1 mmol), samples were taken periodically and immediately analyzed by FTIR spectroscopy.

Acknowledgements

The authors are grateful to the Fundação para a Ciência e a Tecnologia (FCT) for financial support (including Project PTDC/QUI/65427/2006 and post-doctoral grants to C.C.L.P. and S.G.). We also wish to thank the FCT for specific funding toward the purchase of the single-crystal diffractometer. Filomena Gonçalves is acknowledged for the measurement of the elemental analysis data, and Luís Martins is acknowledged for assistance with the FTIR experiments.

Appendix A. Supplementary material

CCDC 703992 contains the supplementary crystallographic data for compound **1**. These data can be obtained free of charge from The Cambridge Crystallographic Data Centre via www.ccdc.cam.ac.uk/data_request/cif. Supplementary data associated with this article can be found, in the online version, at doi:10.1016/j.jorganchem.2009.01.012.

References

[1] (a) M. Abrantes, A.M. Santos, J. Mink, F.E. Kühn, C.C. Romão, Organometallics 22 (2003) 2112;
(b) J. Zhao, A.M. Santos, E. Herdtweck, F.E. Kühn, J. Mol. Catal. A: Chem. 222 (2004) 265;
(c) A.A. Valente, J.D. Seixas, I.S. Gonçalves, M. Abrantes, M. Pillinger, C.C. Romão, Catal. Lett. 101 (2005) 127;
(d) A.M. Martins, C.C. Romão, M. Abrantes, M.C. Azevedo, J. Cui, A.R. Dias, M.T. Duarte, M.A. Lemos, T. Lourenço, R. Poli, Organometallics 24 (2005) 2582;
(e) F.E. Kühn, A.M. Santos, M. Abrantes, Chem. Rev. 106 (2006) 2455;
(f) C. Freund, M. Abrantes, F.E. Kühn, J. Organomet. Chem. 691 (2006) 3718;
(g) M. Pratt, J.B. Harper, S.B. Colbran, Dalton Trans. (2007) 2746;
(h) S.S. Balula, A.C. Coelho, S.S. Braga, A. Hazell, A.A. Valente, M. Pillinger, J.D. Seixas, C.C. Romão, I.S. Gonçalves, Organometallics 26 (2007) 6857.
[2] (a) J. Zhao, E. Herdtweck, F.E. Kühn, J. Organomet. Chem. 691 (2006) 2199;
(b) M. Abrantes, A. Sakthivel, C.C. Romão, F.E. Kühn, J. Organomet. Chem. 691 (2006) 3137.
[3] S. Ebrahim, M. Wills, Tetrahedron: Asymmetr. 8 (1997) 3163.
[4] (a) V.T. Myllymäki, M.K. Lindvall, A.M.P. Koskinen, Tetrahedron 57 (2001) 4629;
(b) E.R. Jarvo, S.J. Miller, Tetrahedron 58 (2002) 2481;
(c) D.R. Kelly, S.M. Roberts, Biopolymers 84 (2006) 74;
(d) E.A.C. Davie, S.M. Mennen, Y. Xu, S.J. Miller, Chem. Rev. 107 (2007) 5759.
[5] (a) M.I. Burguete, M. Collado, E. Gárcia-Verdugo, M.J. Vicent, S.V. Luis, N.G. von Keyserling, J. Martens, Tetrahedron 59 (2003) 1797–1804;;
(b) C. Bolm, M. Kesselgruber, N. Hermanns, J.P. Hildebrand, G. Raabe, Angew. Chem., Int. Ed. 40 (2001) 1488;
(c) M.S. Sigman, E.N. Jacobsen, J. Am. Chem. Soc. 120 (1998) 4901;
(d) M.B. Francis, E.N. Jacobsen, Angew. Chem., Int. Ed. 38 (1999) 937.
[6] (a) F. Le Bideau, M. Salmain, S. Top, G. Jaouen, Chem. Eur. J. 7 (2001) 2289;
(b) D.R. van Staveren, T. Weyhermüller, N. Metzler-Nolte, Organometallics 19 (2000) 3730;
(c) M. Oberhoff, L. Duda, J. Karl, R. Mohr, G. Erker, R. Fröhlich, M. Grehl, Organometallics 15 (1996) 4005;
(d) J.B. Waern, M.H. Harding, Inorg. Chem. 43 (2004) 206.
[7] D. Kunz, R. Fröhlich, G. Erker, Organometallics 20 (2001) 572.
[8] B.E. Mouatassim, H. Elamouri, J. Vaissermann, G. Jaouen, Organometallics 14 (1995) 3296.
[9] (a) M.C. Durrant, S.A. Fairhurst, D.L. Hughes, S.K. Ibrahim, M. Passos, A. Queiros, C.J. Pickett, Chem. Commun. (1997) 2379;
(b) W.M. Harrison, C. Saadeh, S.B. Colbran, D.C. Craig, J. Chem. Soc., Dalton Trans. (1997) 3785;
(c) J. Lauterwein, I.P. Gerothanassis, R.N. Hunston, J. Chem. Soc., Chem. Commun. (1984) 367.
[10] H.D. Flack, Acta Crystallogr. Sect. A 39 (1983) 876.
[11] (a) F.H. Allen, Acta Crystallogr. Sect. B 58 (2002) 380;
(b) F.H. Allen, W.D.S. Motherwell, Acta Crystallogr. Sect. B 58 (2002) 407.
[12] (a) A.M. Martins, R. Branquinho, J.L. Cui, A.R. Dias, M.T. Duarte, J. Fernandes, S.S. Rodrigues, J. Organomet. Chem. 689 (2004) 2368;
(b) R. Lai, J.F. Berthome, I. Lyothier, C. Scheidecker, S. Martin, Inorg. Chim. Acta 350 (2003) 568;
(c) H. Sitzmann, M.D. Walter, G. Wolmershauser, Acta Crystallogr. Sect. E 58 (2002) M777;
(d) M. Tamm, K. Baum, R. Fröhlich, P. Saarenketo, Organometallics 20 (2001) 1376;
(e) R. Lai, A. Archavlis, R. Faure, M. Sanz, J. Chem. Soc., Dalton Trans. (1997) 3259;
(f) R. Lai, S. Martin, Tetrahedron: Asymmetr. 7 (1996) 2783;
(g) R. Fierro, T.E. Bitterwolf, A.L. Rheingold, G.P.A. Yap, L.M. Liable-Sands, J. Organomet. Chem. 524 (1996) 19;
(h) R. Lai, L. Bousquet, A. Heumann, J. Organomet. Chem. 444 (1993) 115;
(i) H.G. Alt, J.S. Han, R.D. Rogers, J. Organomet. Chem. 445 (1993) 115;
(j) P. Jutzi, J. Schnittger, B. Neumann, H.G. Stammler, J. Organomet. Chem. 410 (1991) C13;
(k) R.D. Rogers, J.L. Atwood, M.D. Rausch, D.W. Macomber, J. Crystallogr. Spectrosc. Res. 20 (1990) 555;
(l) W.L. Bell, C.J. Curtis, A. Miedaner, C.W. Eigenbrot, R.C. Haltiwanger, C.G. Pierpont, J.C. Smart, Organometallics 7 (1988) 691;
(m) P.H. Bird, M.R. Churchill, Inorg. Chem. 7 (1968) 349.
[13] (a) H.-U. Blaser, B. Pugin, F. Spindler, J. Mol. Catal. A: Chem. 231 (2005) 1;
(b) S. Gago, J.E. Rodríguez-Borges, C. Teixeira, A.M. Santos, J. Zhao, M. Pillinger, C.D. Nunes, Ž. Petrovski, T.M. Santos, F.E. Kühn, C.C. Romão, I.S. Gonçalves, J. Mol. Catal. A: Chem. 236 (2005) 1;
(c) N. End, A. Pfaltz, Chem. Commun. (1998) 589;
(d) T. Katsuki, J. Mol. Catal. A: Chem. 113 (1996) 87.
[14] (a) A. Al-Ajlouni, A.A. Valente, C.D. Nunes, M. Pillinger, A.M. Santos, J. Zhao, C.C. Romão, I.S. Gonçalves, F.E. Khün, Eur. J. Inorg. Chem. (2005) 1716;
(b) F.E. Kühn, M. Groarke, É. Bencze, E. Herdtweck, A. Prazeres, A.M. Santos, M.J. Calhorda, C.C. Romão, I.S. Gonçalves, A.D. Lopes, M. Pillinger, Chem. Eur. J. 8 (2002) 2370;
(c) L.F. Veiros, A. Prazeres, P.J. Costa, C.C. Romão, F.E. Kühn, M.J. Calhorda, Dalton Trans. (2006) 1383.
[15] A.L. Monteiro, F.K. Zinn, R.F. de Souza, J. Dupont, Tetrahedron: Asymmetr. 8 (1997) 177.
[16] C.A. Gamelas, T. Lourenço, A. Pontes da Costa, A.L. Simplício, B. Royo, C.C. Romão, Tetrahedron Lett. 49 (2008) 4708.
[17] S. Top, J.-S. Lehn, P. Morel, G. Jaouen, J. Organomet. Chem. 583 (1999) 63.
[18] T. Kottke, D. Stalke, J. Appl. Crystallogr. 26 (1993) 615.
[19] APEX2, Data Collection Software, Version 2.1-RC13, Bruker AXS, Delft, The Netherlands, 2006.
[20] CRYOPAD, Remote Monitoring and Control, Version 1.451, Oxford Cryosystems, Oxford, United Kingdom, 2006.
[21] SAINT+, Data Integration Engine, Version 7.23a©, 1997–2005, Bruker AXS, Madison, Wisconsin, USA.
[22] G.M. Sheldrick, SADABS Version 2.01, Bruker/Siemens Area Detector Absorption Correction Program, 1998, Bruker AXS, Madison, Wisconsin, USA.
[23] G.M. Sheldrick, Acta Crystallogr. Sect. A 64 (2008) 112–122.
[24] G.M. Sheldrick, SHELXS-97, Program for Crystal Structure Solution, University of Göttingen, 1997.
[25] G.M. Sheldrick, SHELXL-97, Program for Crystal Structure Refinement, University of Göttingen, 1997.